

Supporting information

Rational Design of MnO/Carbon Nanopeapods with Internal Void Space for High-Rate and Long-Life Li-Ion Batteries

Hao Jiang,[†] Yanjie Hu,[†] Shaojun Guo,^{‡,} Chaoyi Yan,[§] Pooi See Lee,[§] Chunzhong Li^{†,*}*

[†] Key Laboratory for Ultrafine Materials of Ministry of Education, School of Materials Science and Engineering, East China University of Science and Technology, 130 Meilong Road, Shanghai 200237, China

[‡] Physical Chemistry and Applied Spectroscopy, Los Alamos National Laboratory, Los Alamos, New Mexico 87545, United States.

[§] School of Materials Science and Engineering, Nanyang Technological University, Singapore 639798, Singapore.

*Corresponding author: Tel.: +86-21-64250949, Fax: +86-21-64250624

E-mail: czli@ecust.edu.cn (C. Z. Li) and shaojun.guo.nano@gmail.com (S. J. Guo)

1. Figures



Figure S1. Digital photographs of (a) MnO-P NWs, (b) the annealed MnO-P NWs in Ar atmosphere at 500 °C for 3 h and (c) pure MnO NWs.

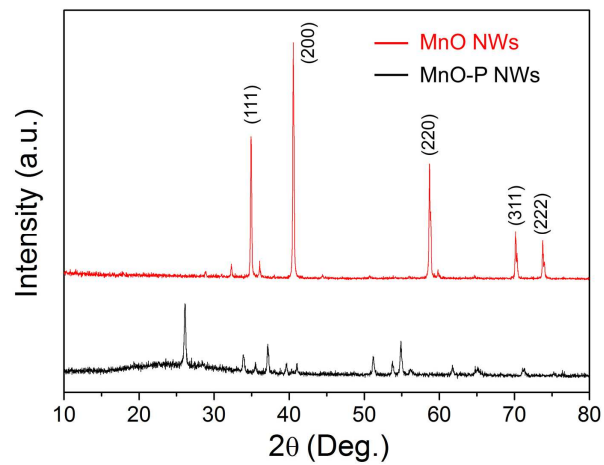


Figure S2. XRD patterns of the MnO-P and MnO NWs.

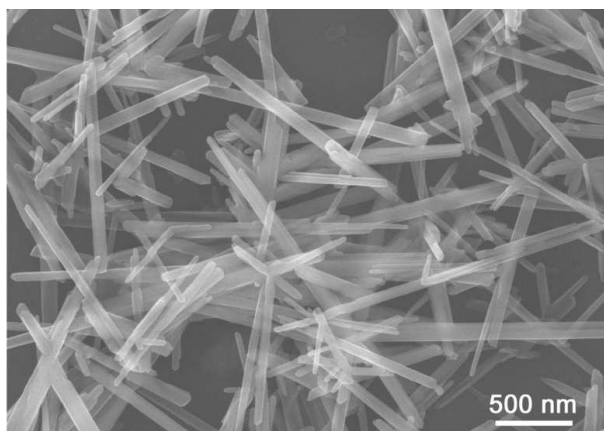


Figure S3. SEM image of the pure MnO NWs.

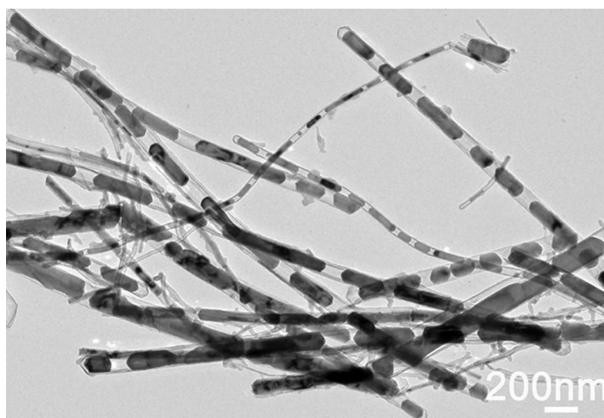


Figure S4. Low-magnification TEM image of the heterostructured MnO/C nanopeapods.

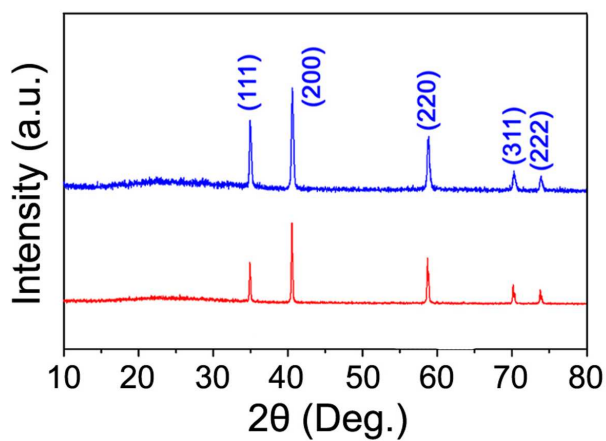


Figure S5. XRD patterns of the as-prepared MnO/C nanopeapods (blue) and MnO/C core/shell NWs (red), respectively.

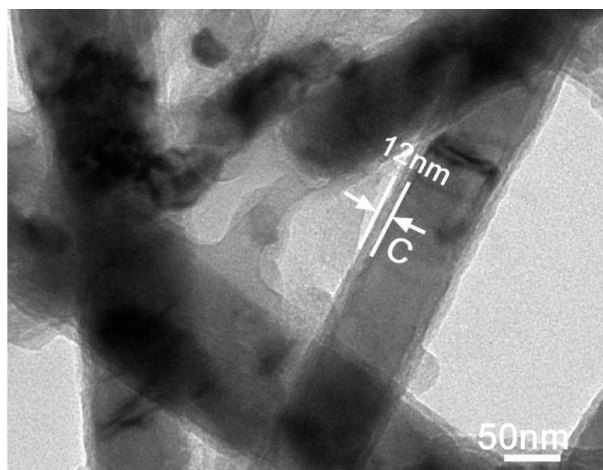


Figure S6. TEM image of the MnO/C core/shell nanowires.

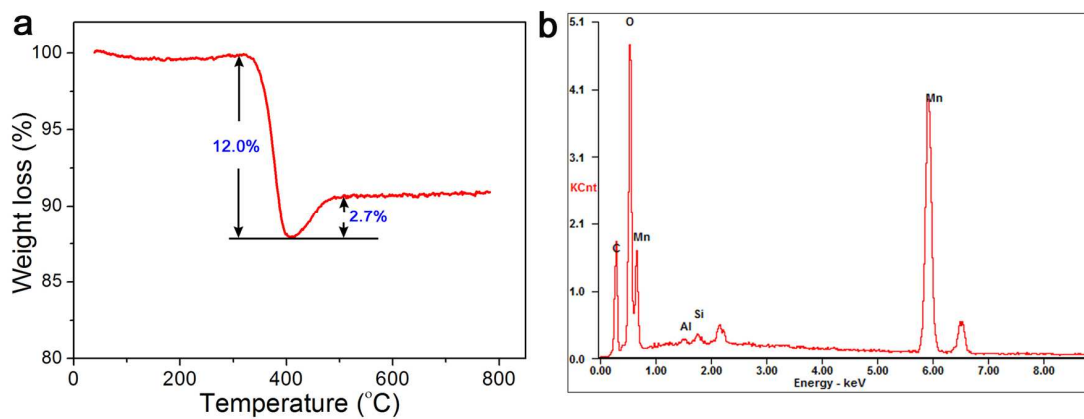


Figure S7. TGA curve and EDS spectrum of the MnO/C nanopeapods. It is well-known that the change of temperature can lead to the variation of the Mn oxidation states, e.g. from 2^{+} to 4^{+} . Among them, Mn_3O_4 is the most stable Mn

oxide due to the spinel-type structure ($\text{Mn}^{2+}(\text{Mn}^{3+})_2\text{O}_4$), which is the final products after annealing at high temperature in air.^{S1} In theory, the oxidation of MnO to Mn_3O_4 can cause 7.5% weight gain. If we assume that the total mass is 100 and carbon content is x, the MnO content is (100-x). From the TG curve, the total weight loss is (12-2.7). Therefore, the following formula is true: $x - 7.5\%(100-x) = 12-2.7$. The result is $x = 15.6$. That is to say, the carbon content is 15.6% in our sample. To further confirm this result, the EDS pattern is also provided, showing a carbon content of 15.0 wt%, which is in good agreement with that from TGA.

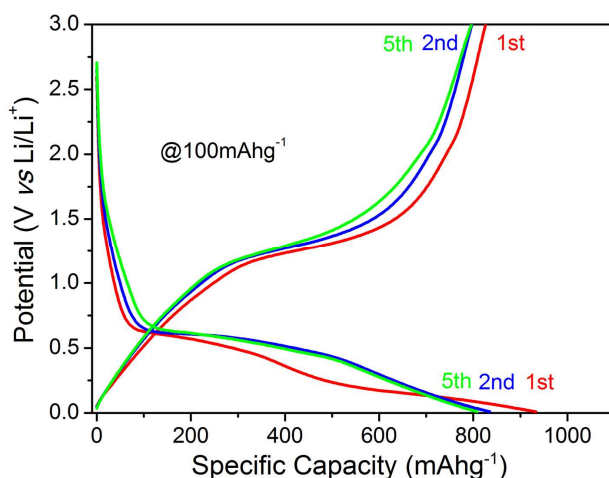


Figure S8. The first five charge/discharge curves of the MnO/C nanopowders showing a high Coulomb efficiency of ~88% at the first cycle.

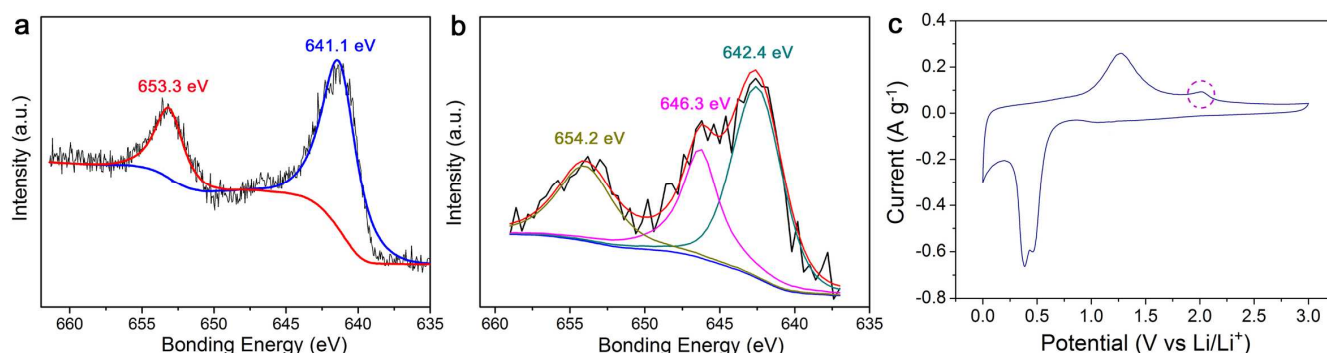


Figure S9. (a, b) High-resolution Mn 2p XPS spectra the MnO/C nanopowders before and after over 1000 cycles. As shown in Figure S9a, the two peaks at 653.3 eV and 641.1 eV are attributed to Mn (II) $2p_{1/2}$ and $2p_{3/2}$, respectively, characteristic of MnO. After over 1000 cycles, the XPS spectrum (Figure S9b) shows the Mn 2p peaks are broader and weaker than the fresh MnO/C nanopowders. Two peaks centered at about 654.2 eV and 642.4 eV, are attributed to Mn^{4+} .^{S2} One peak for Mn (646.3 eV) corresponds to Mn^{2+} .^{S3} To further confirm the fact that the Mn^{2+} ions could be partially re-oxidized to a higher oxidation state, the CV after over 1000 cycles was also tested (Figure S9c). An obvious oxidation peak at ~2.10 V is observed, indicating a higher oxidation state ($> 2^+$) of manganese in the final product.^{28,29}

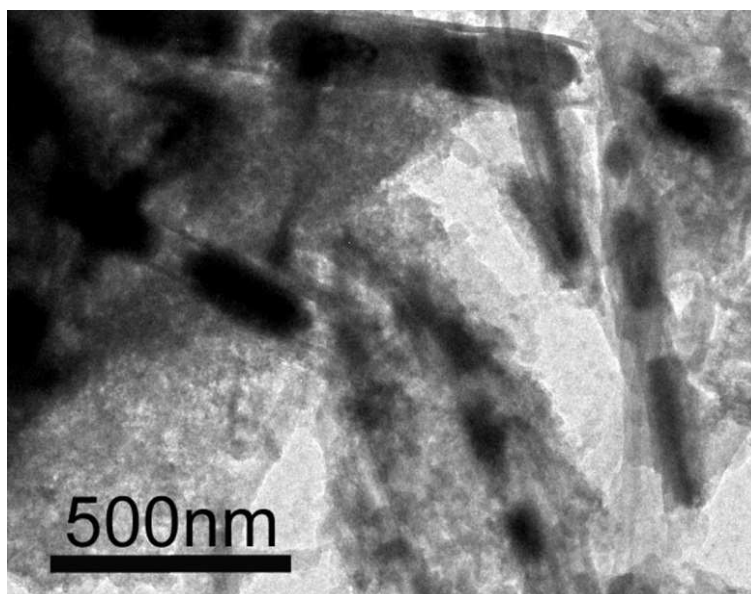


Figure S10. A low magnification TEM image of the MnO/C nanopeapods after over 1000 cycles.

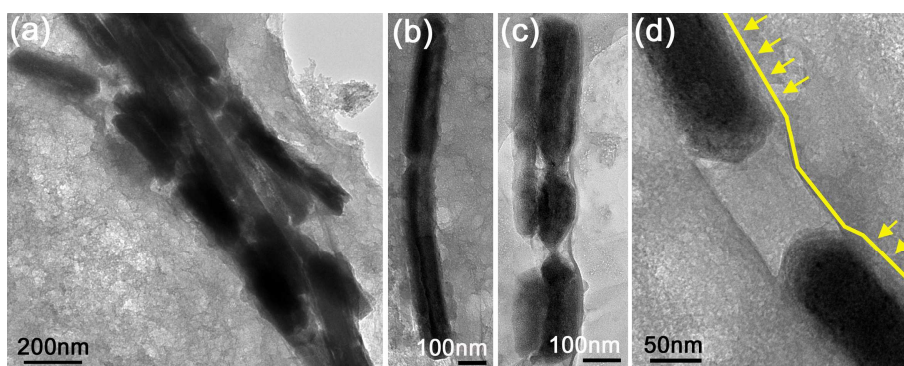


Figure S11. TEM images of the MnO/C nanopeapods after 1000 cycle discharging.

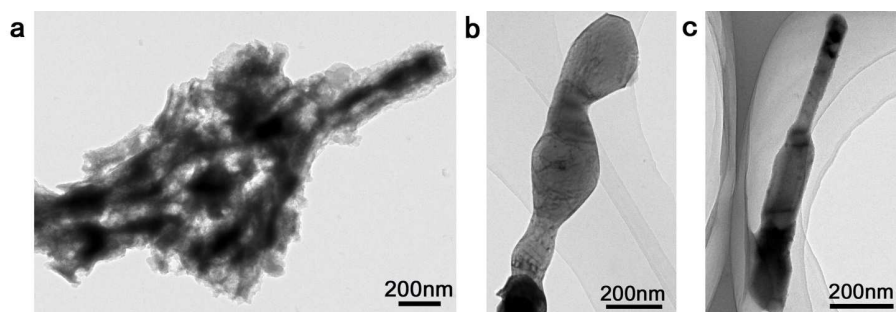


Figure S12. TEM images of (a) MnO/C core/shell NWs and (b, c) MnO NWs after *only* 100 cycles.

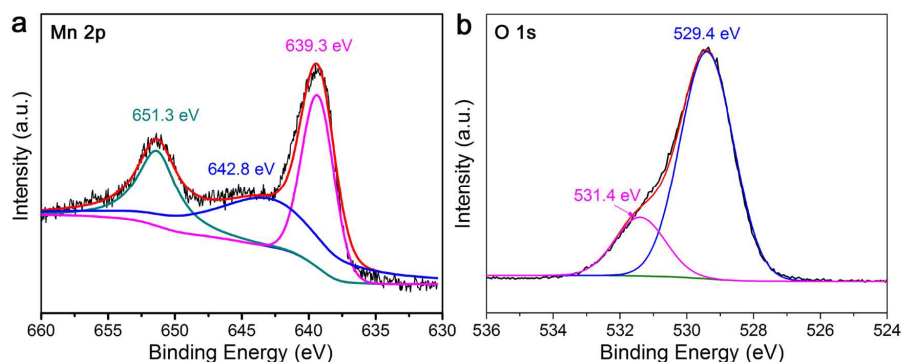


Figure S13. XPS spectra of the MnO/C core/shell NWs after 100 cycles. The appearance of the peak of 642.8 eV (Figure S13a) can be attributed to Mn^{4+} . In Figure S13b, a small O 1s peak at 531.4 eV is observed, indicating the existence of residual O^{2-} species bonded with C atoms in carbon.^{S4} There is no obvious difference between the two samples according to the XPS analysis, indicating that the improvement of cycling stability is mainly related to the unique structure design of MnO/C nanopeapods.

2. Tables

Table S1 Comparison of BET specific surface area of various MnO-based anode materials

Sample	BET specific surface area ($\text{m}^2 \text{g}^{-1}$)	Pore distribution (nm)	Reference
Hollow porous MnO/C microspheres	76.9	11/87	10
MnO/graphene	50.3	2.6	16
MnO@1-D Carbon	64	24.6	27
Porous MnO/C nanotubes	40	7.7	32
MnO/C mesoporous networks	82.7	2.8/7.6	S5
Micro/nanostructured MnO	52.5	20/60	S6
Heterostructured MnO/C nanopeapods	103.0	3.5/11/40	This work

Table S2 Comparison of the electrochemical performance of various MnO-based anode materials

Samples	Current density (mA g ⁻¹)	Reversible capacity (mAh g ⁻¹)	Cycle number (Times)	Capacity retention (%)	Reference
Hollow porous MnO/C microspheres	100	700	50	94	10
MnO/C core-shell nanorods	200	600	40	76	12
Carbon-encapsulated nano-MnO loaded on N-doped carbon webs	1000	1268	700	150	13
Coaxial MnO/C nanotubes	188.9	596	25	84	15
MnO-attached graphene	150	635	20	91	17
MnO/C nanocomposites	75	470	50	64	18
Nitrogen-doped MnO/graphene nanosheets	100	772	90	110	20
Heterostructured MnO/C nanopeapods	500	1018	100	90.0*	This work
	2000	525	1000	86.5*	

* Calculated according to the ratio of the maximum value during cycling process to the last value.

3. References

- S1** Dai, Y. H.; Jiang, H.; Hu, Y. J.; Li, C. Z. Hydrothermal Synthesis of Hollow Mn₂O₃ Nanocones as Anode Material for Li-Ion Battery. *RSC Adv.* **2013**, 3, 19778-19781.
- S2** Xia, H.; Lai, M.; Lu, L. Nanoflaky MnO₂/Carbon Nanotube Nanocomposites as Anode Materials for Lithium-Ion Batteries. *J. Mater. Chem.* **2010**, 20, 6896-6902.
- S3** Castro, V. D.; Ciampi, S. XPS Study of the Growth and Reactivity of FeMnO Thin Films. *Surf. Sci.* **1995**, 331-333, 294-299.
- S4** Schniepp, C. H.; Li, J. L.; McAllister, J. M.; Sai, H.; Herrera-Alonso, M.; Adamson, H. D.; Prud'homme, K. R.; Car, R.; Sacille, A. D.; Aksay, A. I. Functionalized Single Graphene Sheets Derived from Splitting Graphite Oxide. *J. Phys. Chem. B* **2006**, 110, 8535-8539.
- S5** Luo, W.; Xu, X. L.; Sun, Y. M.; Huang, Y. H. Controlled Synthesis of Mesoporous MnO/C Networks by Microwave Irradiation and Their Enhanced-Storage Properties. *ACS Appl. Mater. Interf.* **2013**, 5, 1997-2003.
- S6** Xu, G. L.; Xu, Y. F.; Fang, J. C.; Fu, F.; Sun, H.; Huang, L.; Yang, S. H.; Sun, S. G. Facile Synthesis of Hierarchical Micro/nanostructured MnO Material and Its Excellent Lithium Storage Property and High Performance as Anode in a MnO/LiNi_{0.5}Mn_{1.5}O_{4-δ} Lithium Ion Battery. *ACS Appl. Mater. Interf.* **2013**, 5, 6316-6323.